Mode Discriminator Based on Mode-Selective Coupling

Wenxiang Wang, Yubin Gong, *Member, IEEE*, Guofen Yu, Lingna Yue, and Jiahong Sun

***Abstract*—Mode discriminators based on mode-selective coupling principle have a series of advantages. The designing method of this type of discriminator is presented in this paper. The emphasis is put on the mode-selective coupler with a multihole and multigroup of coupling holes. All of the dimensions of the discriminator are determined by this method. The calibration and power measurement of the discriminator are also investigated. Some design examples of discriminators for 35- and 70-GHz gyrotrons, which can be applied to discriminate the TE_{11}, TE_{01}, and TE_{02} modes and the TE_{01}, TE_{02}, and TE_{03} modes, respectively, are given.**

***Index Terms*—Gyrotron, mode discriminator, mode-selective coupler, multigroup coupling.**

I. Introduction

GYROTRONS usually operate in one high-order TE mode, while vircators excite simultaneously several modes. These types of microwave devices must employ overmoded waveguide as an output circuit. Additionally, the high-power microwave transmission systems of other relativistic devices also need to employ overmoded waveguides to increase the power capacity of the systems. The existence of several modes is unavoidable in an overmoded system. Consequently, discriminating and analyzing the modes in an overmoded waveguide system is needed to know whether the output mode of a microwave source meets the requirement, whether some spurious modes exist, and what the modes are. It is also necessary to use a mode discriminator to appraise the conversion effect of a mode converter. In practice, various mode discrimination methods have been presented [1]–[15].

On the basis that the energy of the microwave field can scorch a piece of paper [1] or change the color of thermosensitive paper [2], or break down the gas in a low pressure cell [3], or illumine a neon tube [4], or heat a dielectric target plate to form an infrared picture [5], the image of an electric field structure can be displayed directly. The advantages of this imaging method are visual, simple, and independent of the microwave frequency. However, a mode discriminator designed according to the image-displaying method is only suitable for a single-mode system. Mode discrimination can also be achieved by comparing the measured pattern with the calculated pattern of the radiated far field of the multimode microwave to determine the mode composition [6]. However, the process of mode discriminating by the far-field analyzing method is complicated, and it is difficult to precisely measure the radiated far-field pattern. Another mode analysis method—the wavenumber spectrometer—which can be applied to *in situ* measurements, is presented by Kasparek and Müller [7] and Barkley *et al.* [8]. A series of small holes as a leaky-wave antenna are milled in the waveguide. The angle θ of the main lobe of the radiation pattern of this antenna depends on the ratio of the wavenumber of the mode in the waveguide to the wavenumber in the free space. Thus, one detects the angle θ by pivoting a parabolic reflector antenna with a rectangular feed horn, the wavenumber spectrum, and then the mode compositions are given. The main shortcoming of this method is that it cannot get the mode composition instantaneously, i.e., cannot measure dynamically. There are some other methods for mode discrimination, e.g., the beat pattern measuring method [9], etc. However, these methods are less applicable and their measuring processes are complicated.

The principle of mode-selective coupling discrimination [10]–[15] is as follows: by coupling a small fraction of the power of one specified mode by a probe or a small hole into the measuring system, while all other modes are uncoupled, one can discriminate the existence of the coupling mode in the main microwave system and its relative intensity according to the output of the coupling power. The advantages of this method are *in situ* and dynamic characteristics, i.e., the mode composition can be observed immediately and continuously, while the microwave system is still connected to the load and is in operation normally. Making use of a mode-selective coupler for mode analysis is one of the most important ways of the mode-selective coupling method. If several mode-selective couplers designed for different desired modes are connected to a microwave system, the mode composition in the system will be determined according to the output of each coupler. In this paper, we will comprehensively introduce the designing method of the mode discriminator based on the mode-selective coupler.

II. Theoretical Basis of the Mode-Selective Coupler

The design of the mode-selective coupler is based on the small-hole coupling theory and the field vector-superposition principle.

A. Small-Hole Coupling

Bethe presented the small-hole diffraction theory in 1944 [16], which is the theoretical basis of calculating small-hole

Manuscript received March 19, 2001; revised November 7, 2001.

The authors are with the National Key Laboratory of High Power Vacuum Electronics, University of Electronic Science and Technology of China, Chengdu, Sichuan 610054, China (e-mail: wxwang@uestc.edu.cn).

Digital Object Identifier 10.1109/TMTT.2002.806947

coupling. Bethe's work indicates that the coupling of a small hole can be equivalent to an electric dipole and a magnetic dipole. In the sub-arm of a coupler, the amplitude of the traveling wave excited by a mode in the main arm of the coupler is directly proportional to the polarizability of the equivalent dipole, the normal component of the electric field, and the tangential components of the magnetic field in the main arm at the small-hole position. It is also proportional to the corresponding field components of the excited mode in the sub-arm at the same position [17].

Generally, the main arm of a mode-selective coupler is an overmoded circular or rectangular waveguide. For measurement convenience, the sub-arm of the coupler is usually a rectangular waveguide working in the fundamental mode (TE_{10}). Assuming that $v^{\pm}$, called the coupling intensity of a single hole, represents the relative amplitude of the TE_{10} mode excited in the sub-waveguide by the (m, n) mode in the main waveguide through a single circular hole, and the upper sign of "$\pm$" in $v^{\pm}$ indicates the $+z$-direction and the lower indicates the $-z$-direction. When the coupling occurs between two different types of waveguide, the ratio of the power, rather than the amplitude of the (m, n) mode to the TE_{10} mode, which is presented in [13], should be calculated to derive the $v^{\pm}$. Thus, according to Bethe's theory [16], [17], expressions of $v^{\pm}$ can be achieved for various coupling from the TE_{mn} or TM_{mn} modes in the circular or rectangular overmoded waveguide to the TE_{10} mode in the sub-waveguide. When calculating $v^{\pm}$, the large-hole factors and thickness factors of the electric and magnetic dipoles should be taken into account [18].

B. Field Vector Superposition

All of the wave functions can be expressed as complex vectors of their amplitudes and phases. The superposition of two or more vectors depends not only on their amplitudes, but also on their phase relation. This vector-superposition principle is also one of the design fundamentals for any multielement coupler [19], [20].

We assume that each coupling hole is so small that the coupling through it will have no influence on the fields in the main waveguide and the propagation constants in the sub-waveguide; in other words, the amplitude of the incident wave will be unaltered in the whole coupling region.

Supposing there are $N = 2n$ or $N = 2n + 1$ coupling holes distributed symmetrically and the origin of the coordinate system is at the symmetrical center [see Fig. 1 (a) and (b)], the single hole coupling intensity for each pair of holes is $v_0^{\pm}, v_1^{\pm}, v_2^{\pm}, \ldots, v_k^{\pm}, \ldots, v_n^{\pm}$, respectively, the incident wave propagates along the $+x$-direction in the main waveguide and its phase constant is β_2, and the phase constant of the excited wave in the sub-waveguide is β_1. The total relative amplitude of the wave coupled into the sub-waveguide will then be

$$V^{\pm} = v_0^{\pm} + 2\left|\sum_{k=1}^{n} v_k^{\pm}\cos\theta_k^{\pm}\right|, \qquad v_0^{\pm} = 0 \text{ for } N = 2n; \quad v_0^{\pm} \neq 0 \text{ for } N = 2n+1 \tag{1}$$

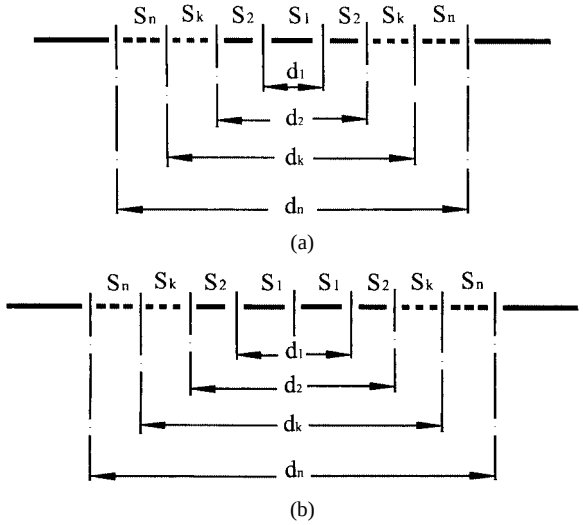

Fig. 1. Multihole coupling. (a) The number of coupling holes $N = 2n$. (b) The number of coupling holes $N = 2n + 1$.

where

$$\begin{cases} \theta_k^{\pm} = (\beta_1 \mp \beta_2)d_k/2 \\ d_k = \begin{cases} S_1 + 2\sum_{k=2}^{n} S_k, & \text{for } N = 2n \\ 2\sum_{k=1}^{n} S_k, & \text{for } N = 2n+1. \end{cases} \end{cases} \tag{2}$$

In order to obtain constructive interference, it should be satisfied that

$$\theta_k = (2i_k - l)\pi, \qquad i_k = 1, 2, \ldots; \quad l = 0 \text{ or } l = 1 \text{ alternatively.} \tag{3}$$

Under this condition, the terms in (1) will be added up directly. In order to obtain destructive interference, the most convenient method is to make all terms in (1) equal to zero, i.e.,

$$\theta_k = (i_k - 1/2)\pi, \qquad i_k = 1, 2, \ldots. \tag{4}$$

1) Equal-Interval Coupling: If all the distances between adjacent coupling holes are equal to S for multihole coupling, i.e.,

$$d_k = (2k - g)S, \qquad k = 1, 2, \ldots, n; \quad g = 1 \text{ for } N = 2n; \quad g = 0 \text{ for } N = 2n+1 \tag{5}$$

then

$$\begin{cases} \theta_k^{\pm} = (2k - g)\varphi^{\pm} \\ \varphi^{\pm} = (\beta_1 \mp \beta_2)S/2 \end{cases}, \quad k = 1, 2, \ldots, n; \quad g = 1 \text{ for } N = 2n; \quad g = 0 \text{ for } N = 2n+1 \tag{6}$$

and now

$$V^{\pm} = v_0^{\pm} + 2\left|\sum_{k=1}^{n} v_k^{\pm}\cos(2k - g)\varphi^{\pm}\right|, \quad v_0^{\pm} = 0; \quad g = 1 \text{ for } N = 2n; \quad v_0^{\pm} \neq 0; \quad g = 0 \text{ for } N = 2n+1. \tag{7}$$

Comparing (6) with (3), it can be seen that constructive interference will occur under the condition

$$\varphi^{\pm} = i\pi, \qquad i = 1, 2, \ldots \tag{8}$$

and the condition for destructive interference is

$$\varphi^{\pm} = (i - 1/2)\pi, \qquad i = 1, 2, \ldots. \tag{9}$$

2) Equal-Intensity Coupling: If all the radii of the coupling holes are equal, the coupling intensity will also be identical for all the holes, i.e.,

$$v_0^{\pm} = v_1^{\pm} = v_2^{\pm} = \cdots = v_k^{\pm} = \cdots = v_n^{\pm} = v^{\pm}. \tag{10}$$

Hence,

$$V^{\pm} = v^{\pm}\left(K + 2\left|\sum_{k=1}^{n}\cos\theta_k^{\pm}\right|\right), \qquad K = 0 \text{ for } N = 2n; \quad K = 1 \text{ for } N = 2n+1 \tag{11}$$

and conditions (3) and (4) are also suitable for equal-intensity coupling.

3) Equal-Interval and Equal-Intensity Coupling: Replacing $\theta_k^{\pm}$ in (11) by that in (6), we obtain

$$V^{\pm} = v^{\pm}\left|\frac{\sin N\varphi^{\pm}}{\sin\varphi^{\pm}}\right|. \tag{12}$$

III. Design of the Mode-Selective Coupler

In the following discussions, the mode, which needs to be coupled to the sub-arm from the main arm, is called the coupled mode (desired mode), and the modes that should not be coupled are called the uncoupled modes (unwanted modes). The task of designing the mode-selective coupler is to enhance the coupling intensity of the coupled mode and counteract the coupling of unwanted modes in the positive direction. If we design several couplers for different modes (in practice, we only need to set up several coupling arms on the same main waveguide), it can be detected which modes exist in the main waveguide and how much their relative intensities are. Obviously, this judgment is independent of the backward wave in the sub-arm. Thus, the backward wave, in other words, the directivity of the coupler, must not to be taken into account when designing the mode-selective coupler when a match load is connected to the backward terminal of the sub-arm of each mode coupler. The design of mode-selective couplers is simpler than that of the mode-selective directional couplers. The following discussion about the mode discriminator will only involve forward waves, but the principle and design method presented here is also suitable for mode-selective directional couplers.

A. Determination of the Distance Between Holes

It can be seen from the above section that the in-phase constructive interference and out-of-phase destructive interference of the mode-selective coupler depend on the phase shift of the electromagnetic wave between holes. In other words, it depends on the interval between holes for a given waveguide and mode.

All the parameters for the coupled mode are represented by subscription "w," and for the unwanted modes expressed by subscription "u." The condition for in-phase constructive interference can be obtained from (3)

$$d_{w,k} = (2i_{w,k} - l)\left|\frac{\lambda_w\lambda_{10}}{\lambda_w - \lambda_{10}}\right|, \qquad i_{w,k} = 1, 2, \ldots; \quad k = 1, 2, \ldots, n; \quad l = 0 \text{ or } l = 1 \text{ alternatively} \tag{13}$$

here, λ_w is the guide wavelength of the coupled mode in the main waveguide and λ_{10} is that of the TE_{10} mode in the rectangular sub-waveguide.

Condition (4) for out-of-phase destructive interference must be satisfied to suppress an unwanted mode, i.e.,

$$d_{u,k} = (i_{u,k} - 1/2)\left|\frac{\lambda_u\lambda_{10}}{\lambda_u - \lambda_{10}}\right|, \qquad i_{u,k} = 1, 2, \ldots; \quad k = 1, 2, \ldots, n \tag{14}$$

λ_u is the guide wavelength of the unwanted mode in the main waveguide.

In the case of equal-interval coupling, the conditions of in-phase constructive interference and out-of-phase destructive interference can be written from (8) and (9), respectively, as follows:

$$S_w = i_w\left|\frac{\lambda_w\lambda_{10}}{\lambda_w - \lambda_{10}}\right|, \qquad i_w = 1, 2, \ldots \tag{15}$$

$$S_u = (i_u - 1/2)\left|\frac{\lambda_u\lambda_{10}}{\lambda_u - \lambda_{10}}\right|, \qquad i_u = 1, 2, \ldots. \tag{16}$$

B. Installation of Multigroup Coupling Holes

Considering not only the enhancement of the amplitude of the coupled mode, but also the suppression of the amplitude of the unwanted modes, d_k or S must satisfy two equations simultaneously, such as (13) and (14) or (15) and (16). This is very difficult for unequal interval coupling because all of the $d_k(k = 1, 2, \ldots, n)$ must satisfy these two conditions. In addition, if two, three, or even more modes need to be suppressed, the interval S will be required to satisfy three, four, or even more equations simultaneously, which is almost impossible. The installation of multigroup coupling holes can solve this problem. At first, we design the interval d_k or S in the first group, which satisfies one equation (the enhancing condition for the coupled mode) or two equations (adding the suppressing condition for one unwanted mode). Next, we set up the second group of coupling holes with the same interval S and radii, corresponding one by one to the holes in the first group. However, there is a displacement S_{p1} between the two groups, and the displacement must satisfy the suppression condition (16) for one or two unwanted modes. Depending on how many unwanted modes need to be suppressed, the third, the fourth group of holes, etc. may be needed. For each new additional group, the number of coupling holes should be equal to that of the total original groups, e.g., the holes of the third group should repeat the holes of the first and the second groups with new displacement S_{p2}. The holes'

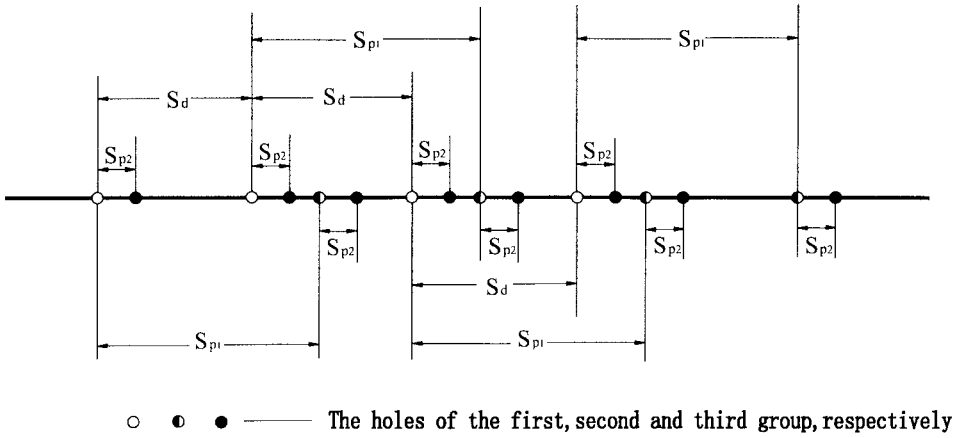

Fig. 2. Hole distribution of a coupler with three-group coupling holes.

intervals and radii must also be identical with those of the corresponding holes in the original groups, but move wholly a new displacement S_{p2}, S_{p3}, ... Fig. 2 shows the hole distribution of a three-group coupler. The total number of coupling holes (N_T) will increase exponentially with the number of groups m, i.e.,

$$N_T = 2^{(m-1)} \times N_1 \tag{17}$$

where N_1 is the number of coupling holes in the first group. The length of the coupling region is

$$L = (N_1 - 1)S_w + \sum_{g=1}^{m-1} S_{p,g} \tag{18}$$

$S_{p,g}$ should be derived according to (16) for each group. With the installation of a new group of coupling holes, another one or two unwanted mode can be suppressed. Thus, the total relative amplitude for multigroup coupling holes is

$$\begin{cases} V^{\pm} = \left| v_0^{\pm} + 2\sum_{k=1}^{n} v_k^{\pm} \cos\theta_k^{\pm} \right| \left| \prod_{g=1}^{m-1} \cos\theta_g^{\pm} \right|, \\ \theta_g^{\pm} = (\beta_{10} \mp \beta_2) S_{p,g}/2 \end{cases}$$
$$v_0^{\pm} = 0 \text{ for } N = 2n; \quad v_0^{\pm} \neq 0 \text{ for } N = 2n+1. \tag{19}$$

Notice that $\theta_k^{\pm}$ in (19) should be calculated according to (2), and $\beta_1 = \beta_{10}$, $\beta_2 = \beta_{w,g}$ for the coupled mode and $\beta_2 = \beta_{u,g}$ for the unwanted mode in the expressions of $\theta_k^{\pm}$ and $\theta_g^{\pm}$.

The number of the groups of coupling holes depends on the number of unwanted modes that need to be suppressed in the microwave system. Obviously, installing too many groups of coupling holes is unrealistic because the multigroup installation results in not only increasing exponentially the number of coupling holes (so that the length of the coupler rises quickly), but also causing unavoidably the overlap of the holes. Consequently, the 2∼4 groups of coupling holes should be employed, and the following factors need to be considered.

1) When determining $S_{p,g}$, the $i_{u,g}$ should be chosen carefully. If possible, $\lambda_{u,g}$ and λ_{10} should be adjusted to change $S_{p,g}$ so that we can choose one value of $S_{p,g}$ suitable for suppression conditions of two unwanted modes and reducing the group number of coupling holes.
2) The unwanted modes should be taken into account in order according to their magnitudes in the main waveguide and the degree of their influence on the coupling of the coupled mode. Usually, the closer the waveguide wavelength of one mode is to that of the lowest mode excited in the system or to that of the coupled mode, the easier this mode will be excited and the more it will influence the coupling of the coupled mode. Thus, these modes should be suppressed first when designing the groups of coupling holes.
3) It is especially important to notice that the value of $S_{p,g}$ should avoid being close to $(i - 1/2)S_w$ $(i = 1, 2, \ldots)$ because the forward coupling wave of the coupled mode will be counteracted if $S_{p,g}$ is equal to $(i - 1/2)S_w$. Under the condition that the overlap of the holes will not occur, the closer $S_{p,g}$ is to an integer multiple of S_w, the better it is.

C. Determination of Waveguide Dimensions

The dimensions of the main waveguide of the mode-selective coupler can be determined according to the power capacity and propagating condition of the mode in the system. The propagating condition can be written as follows for overmoded circular waveguides:

$$\lambda_1 \leq 2\pi R/\chi_{mn} \tag{20}$$

and for overmoded rectangular waveguides

$$\lambda_1 \leq 2\Big/\sqrt{\left(\frac{m}{A}\right)^2 + \left(\frac{n}{B}\right)^2} \tag{21}$$

where m, n are the eigennumbers of the highest mode propagating in the systems and λ_1 is the largest guide wavelength in the operating passband. χ_{mn} is the nth root of the first kind of mth-order Bessel function (TM mode) or its derivative (TE mode). R represents the radius of the circular main waveguide and A, B are the wide wall and narrow wall of the rectangular main waveguide.

It should be noted that the increase of the main-waveguide dimensions can lead to the increase of high-order modes, but the proper increase of the dimension R or A will be good for the extension of the passband of the coupler. The values of R

and A should be readjusted according to requirements 1) and 2) in Section III-B.

After the values of R and A have been determined, the broad wall dimension a of the sub-waveguide in the case of equal-interval coupling can be decided according to both (15) and (16) to enhance greatly the forward wave of the coupled mode and suppress completely the forward wave of one unwanted mode. Thus, from (15) and (16), we obtain

$$\lambda_{10,0}=\begin{cases}\dfrac{[i_w-(i_u-1/2)]\lambda_w\lambda_u}{i_w\lambda_w-(i_u-1/2)\lambda_u}, \\ \quad (\lambda_w-\lambda_{10})(\lambda_u-\lambda_{10})>0 \\ \dfrac{[i_w+(i_u-1/2)]\lambda_w\lambda_u}{i_w\lambda_w+(i_u-1/2)\lambda_u}, \\ \quad (\lambda_w-\lambda_{10})(\lambda_u-\lambda_{10})<0\end{cases} \tag{22}$$

where the subscription "0" refers to the parameters at the center operating frequency of the coupler. Thus, a can be derived from $\lambda_{10,0}$ and should be fit for the propagating condition of only TE_{10} mode

$$\lambda_2>a>\lambda_1/2 \tag{23}$$

where λ_2 is the minimal wavelength in the operating passband.

The narrow wall dimension b of the sub-waveguide can usually be the size of a standard waveguide because $\lambda_{10,0}$ is independent of b.

D. Calculation of the Radius of Coupling Hole

In the case of equal-intensity coupling, (19) can be written as

$$V^{\pm}=v^{\pm}\left|K+2\sum_{k=1}^{n}\cos\theta_k^{\pm}\right|\left|\prod_{g=1}^{m-1}\cos\theta_g^{\pm}\right|, \quad K=0 \text{ for } N=2n;\quad K=1 \text{ for } N=2n+1. \tag{24}$$

Notice that, to calculate $V^{\pm}$, $v^{\pm}$ must be derived first. For this reason, we assume that the required coupling coefficient for the coupled mode at the center operating frequency of the mode-selective coupler is C_0 (in decibels). The coupling intensity of the single hole at the center frequency for the forward wave is then

$$v_{w,0}^{\pm}=10^{C_0/20}\Big/\left|K+2\sum_{k=1}^{n}\cos\theta_{w,k}^{\pm}\right|\left|\prod_{g=1}^{m-1}\cos\theta_{w,g}^{\pm}\right|, \quad K=0 \text{ for } N=2n;\quad K=1 \text{ for } N=2n+1. \tag{25}$$

Starting with the above equation, according to the theory of small-hole coupling (Section II-A), the radius r_0 of the coupling hole can be derived for the case of equal-intensity coupling. Therefore, the relative amplitude coupled into the sub-arm of the mode-selective coupler at any frequency can be calculated by (24) for both the forward and backward wave, including both coupled and unwanted modes.

To calculate the radii of the coupling holes in the case of unequal intensity and the case of unequal-interval distribution, the relation of the coupling intensity of each pair of holes may be derived according to some coupling functions [21] such as the cosine function, triangular function, and Chebyshev polynomial or binomial distribution.

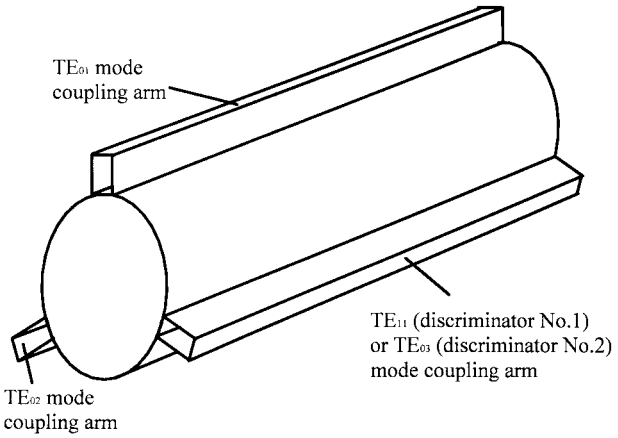

Fig. 3. Three-arm mode discriminator.

E. Parameters of a Mode-Selective Coupler

From the above discussions, the parameters of a mode-selective coupler for equal-intensity coupling can be derived. The coupling coefficient C of a coupled mode is

$$C=-20\lg A_w^{+}=-20\lg v_w^{+}\left|K+2\sum_{k=1}^{n}\cos\theta_{w,k}^{+}\right|-20\lg\left|\prod_{g=1}^{m-1}\cos\theta_{w,g}^{+}\right|, \quad K=0 \text{ for } N=2n;\quad K=1 \text{ for } N=2n+1. \tag{26}$$

The suppression of the unwanted mode is

$$p=20\lg\frac{A_w^{+}}{A_u^{+}}=20\lg\frac{v_w^{+}\left|K+2\sum_{k=1}^{n}\cos\theta_{w,k}^{+}\right|}{v_u^{+}\left|K+2\sum_{k=1}^{n}\cos\theta_{u,k}^{+}\right|}+20\lg\frac{\left|\prod_{g=1}^{m-1}\cos\theta_{w,g}^{+}\right|}{\left|\prod_{g=1}^{m-1}\cos\theta_{u,g}^{+}\right|}, \quad K=0 \text{ for } N=2n;\quad K=1 \text{ for } N=2n+1. \tag{27}$$

The coupling coefficient of the unwanted mode is

$$C_u=-20\lg A_u^{+}=C+p. \tag{28}$$

IV. Calibration of and Power Measurement by a Mode Discriminator

The coupling arms designed for different coupled modes are connected to the main waveguide of the mode discriminator. A power meter or diode is connected to the forward output port of each arm and a match load is required for each backward output port. After calibrating the coupling coefficient of the coupled mode and the suppression of the unwanted modes for each arm, the mode composition and the power of each mode in the system can be determined by measuring the forward output of each coupling arm.

TABLE I
CALCULATED RESULTS FOR THREE DESIGNING EXAMPLES

Parameters \ Discriminator		No.1			No.2		
		TE_{01} coupling arm	TE_{02} coupling arm	TE_{11} coupling arm	TE_{01} coupling arm	TE_{02} coupling arm	TE_{03} coupling arm
Given parameters	f_0 (GHz)	35.0			70.0		
	C_0 (dB)	30			30		
	R (mm)	10.0			13.9		
	b (mm)	3.56			1.88		
Designed dimensions	a (mm)	5.51	5.74	6.34	3.10	2.92	2.77
	S_w (mm)	38.18	22.91	37.15	16.51	16.51	18.54
	S_p (mm)	12.61	17.17	9.61	14.88	11.44	7.06
	r_0 (mm)	1.55	1.37	1.61	1.01	1.0	0.99
	n	3	3	3	3	3	3
	N_T	12	12	12	12	12	12
	L (mm)	203.51	129.25	195.36	97.43	93.99	99.76
Calculated suppressions in (dB) at f_0	TE_{01}		77.23	63.38		45.12	47.57
	TE_{02}	62.68		60.90	40.33		63.36
	TE_{03}				57.16	57.00	
	TE_{11}	78.10	97.21		5.98	19.76	31.45
	TE_{21}	5.67	8.57	2.98	0.90	15.46	29.87
	TE_{31}	11.26	15.52	9.64	5.76	2.58	28.20
	TE_{41}	0.80	17.89	5.98	4.01	1.53	36.07
	TE_{51}	5.83	20.36	1.77	8.41	5.93	29.70
	TE_{12}	3.53	8.90	0.68	3.16	19.23	31.27
	TE_{22}	0.94	25.37	7.69	4.39	-0.85	30.19

For calibrating the mode discriminator, it is necessary to excite each coupled and unwanted mode because the measurement of the coupling coefficient and suppression must be done for an individual mode. However, an individual exciter of each mode, except for some simple lower order modes, is not available yet. Thus, direct measurement of the coupling coefficient and suppression are impossible. Making use of the exchangeability of the mode discriminator as a linear component, we can approximately solve this problem by employing two identical mode discriminators. For simplicity, we take two identical discriminators, I and II, which both have two coupling arms, as an example to explain the calibrating principle of this method. Assume the coupled modes of the coupling arms are M_1 and M_2, respectively. For the M_1 mode coupling arm, the coupling coefficient in the forward direction is C_{11}, and the suppression to the M_2 mode in the same direction is p_{12}. For the M_2 mode coupling arm, the coupling coefficient is C_{22}, and the suppression to M_1 mode is p_{21}. Obviously, according to the definition of the discriminator's parameters in Section III-E, the coupling coefficient of the M_2 mode in the M_1 mode coupling arm is $C_{11}+p_{12}$, and that of the M_1 mode in the M_2 mode coupling arm is $C_{22}+p_{21}$.

The main waveguides of two identical discriminators are connected to each other and terminated with match loads. The mode discriminator I acts as the exciting device and the discriminator II is the measured device. When the input power P_{in} of TE_{10} mode is injected into discriminator I through the M_1 mode coupling arm, the modes higher than M_2 will not be excited since the main waveguide is cutoff for all of these modes. The excited power of the M_1 mode and M_2 mode in the main waveguide, respectively, are

$$\left.\begin{aligned} P'_{11} &= 10^{-(C_{11}/10)}P_{\text{in}} \\ P'_{12} &= 10^{-((C_{11}+p_{12})/10)}P_{\text{in}} \end{aligned}\right\}. \tag{29}$$

These two modes propagate along the forward direction into discriminator II, and a part of the power will be coupled into the M_1 and M_2 mode coupling arms of discriminator II. The output powers of the two coupling arms, respectively, are

$$\left.\begin{aligned} P_{11} &= 10^{-(C_{11}/10)}P'_{11} + 10^{-((C_{11}+p_{12})/10)}P'_{12} \\ P_{12} &= 10^{-(C_{22}/10)}P'_{12} + 10^{-((C_{22}+p_{21})/10)}P'_{11} \end{aligned}\right\}. \tag{30}$$

When P_{in} is injected into discriminator I through the M_2 mode coupling arm, similarly, the excited power in the main wave-

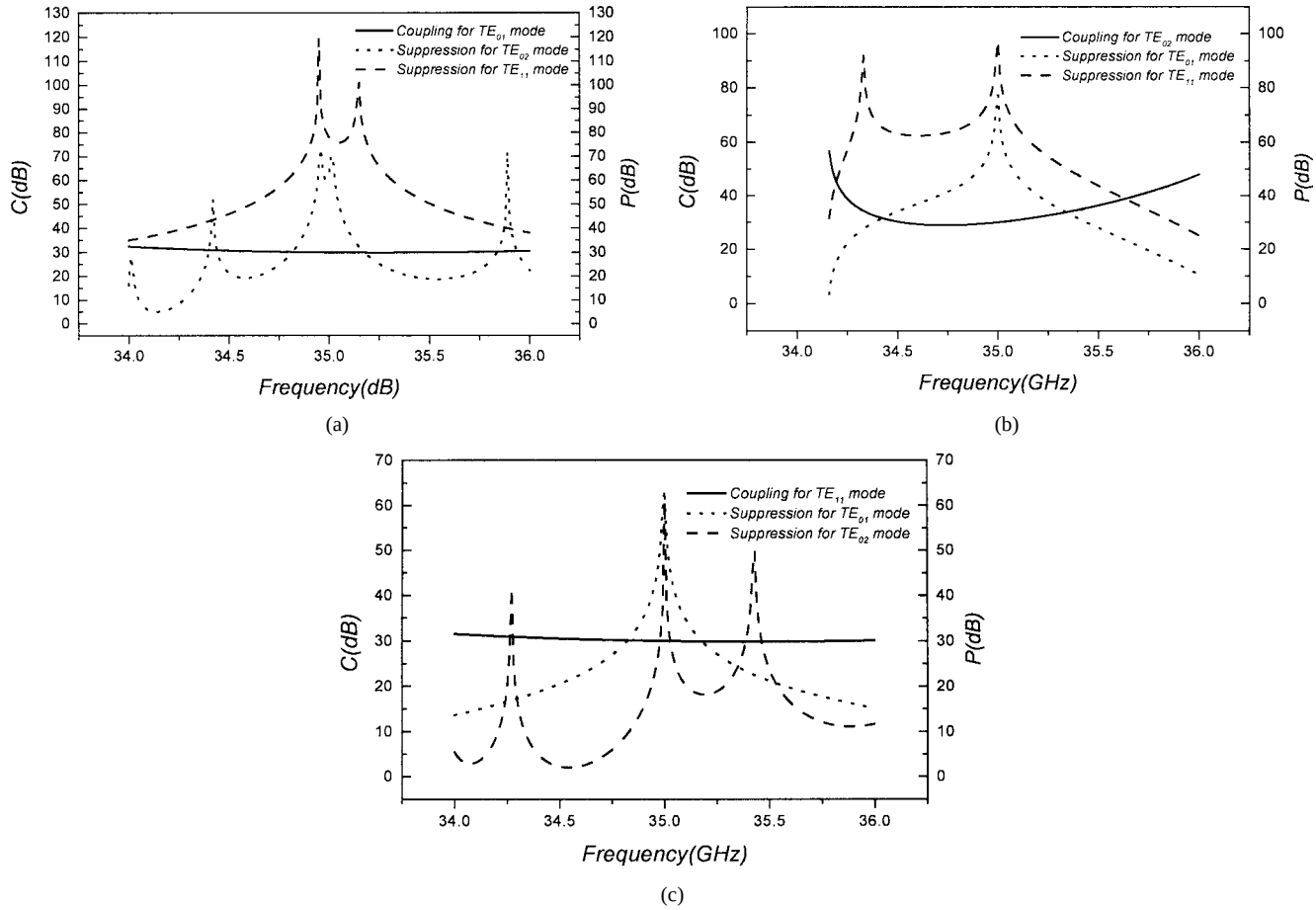

Fig. 4. Relations of coupling and suppression versus frequency for design example no. 1. (a) TE_{01} mode coupling arm. (b) TE_{02} mode coupling arm. (c) TE_{11} mode coupling arm.

guide are

$$\left.\begin{aligned} P'_{21} &= 10^{-((C_{22}+p_{21})/10)}P_{\mathrm{in}} \\ P'_{22} &= 10^{-(C_{22}/10)}P_{\mathrm{in}} \end{aligned}\right\} \tag{31}$$

and the output powers from the M_1 and M_2 mode coupling arms of discriminator II, respectively, are

$$\left.\begin{aligned} P_{21} &= 10^{-(C_{11}/10)}P'_{21} + 10^{-((C_{11}+p_{12})/10)}P'_{22} \\ P_{22} &= 10^{-(C_{22}/10)}P'_{22} + 10^{-((C_{22}+p_{21})/10)}P'_{21} \end{aligned}\right\}. \tag{32}$$

Thus, we obtain

$$\left.\begin{aligned} P_{11}/P_{\mathrm{in}} &= 10^{-(C_{11}/5)}\left(1+10^{-(p_{12}/5)}\right) \\ P_{22}/P_{\mathrm{in}} &= 10^{-(C_{22}/5)}\left(1+10^{-(p_{21}/5)}\right) \\ P_{12}/P_{\mathrm{in}} &= P_{21}/P_{\mathrm{in}} \\ &= 10^{-((C_{11}+C_{22})/10)}\left(10^{-(p_{12}/10)}+10^{-(p_{21}/10)}\right) \end{aligned}\right\}. \tag{33}$$

Now, there are three independent equations for four unknowns C_{11}, C_{22}, p_{12}, and p_{21}. We use iteration method to solve this problem. As the first step, we assume $p_{12} = p_{21}$, then the third equation of (33) can be rewritten as

$$\left.\begin{aligned} P_{12}/P_{\mathrm{in}} &= 2\times 10^{-((C_{11}+C_{22}+p_{21})/10)} \\ P_{21}/P_{\mathrm{in}} &= 2\times 10^{-((C_{11}+C_{22}+p_{12})/10)} \end{aligned}\right\}. \tag{34}$$

Replacing the third equation of (33) by (34), we now have four independent equations. The parameters P_{11}/P_{in}, P_{22}/P_{in}, P_{12}/P_{in}, and P_{21}/P_{in} in these four equations can be determined by measurement. Thus, the first approximations for C'_{11}, C'_{22}, p'_{12}, and p'_{21} can be derived. Next, assuming the second approximation $p''_{21} = p''_{12} + \Delta p'$, here, $\Delta p' = p'_{21} - p'_{12}$, the unknown number will become three. Using the measured data and (33) again, the second approximations for C''_{11}, C''_{22}, and p''_{12} can be derived. Then, assuming the third approximation $p'''_{21} = p'''_{12} + \Delta p''$, and $\Delta p'' = p''_{21} - p''_{12}$, C'''_{11}, C'''_{22}, p'''_{12} can be obtained. Repeat this procedure until Δp is a stable constant to obtain final C_{11}, C_{22}, p_{12}, and p_{21}.

When C_{11}, C_{22}, p_{12}, and p_{21} are all known, the calibrated discriminator can be employed for mode discrimination and power measurement. Assuming the main waveguide of this discriminator is connected to a microwave system, the propagating power of M_1 and M_2 modes in this system are P_{01} and P_{02}, respectively, and the measured power at the forward output ports of the M_1 mode coupling arm and M_2 mode coupling arm of this discriminator are P_1 and P_2, respectively, we obtain

$$\left.\begin{aligned} P_1 &= 10^{-(C_{11}/10)}P_{01} + 10^{-((C_{11}+p_{12})/10)}P_{02} \\ P_2 &= 10^{-(C_{22}/10)}P_{02} + 10^{-((C_{22}+p_{21})/10)}P_{01} \end{aligned}\right\}. \tag{35}$$

Hence, P_{01} and P_{02} can be determined from the measured data P_1 and P_2, and the total power propagating in the system is $(P_{01} + P_{02})$.

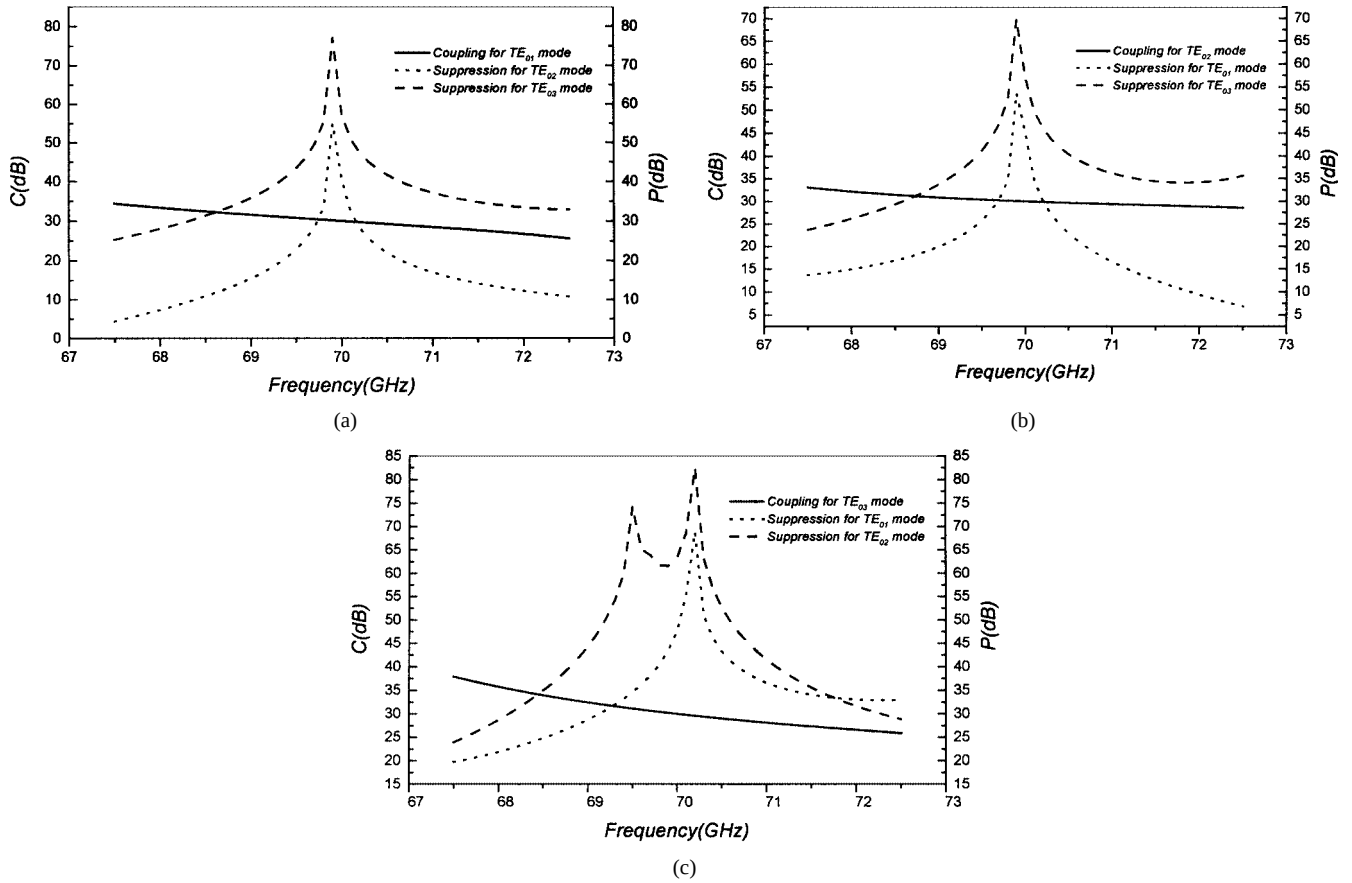

Fig. 5. Relations of coupling and suppression versus frequency for design example no. 2. (a) TE_{01} mode coupling arm. (b) TE_{02} mode coupling arm. (c) TE_{03} mode coupling arm.

When there are more modes in the system and more coupling arms on the mode discriminator, the calibration and power measurement can be done similarly.

V. Design Examples

Following the above method, we have designed some discriminators with equal-interval and equal-intensity coupling for two gyrotrons. Fig. 3 gives the structure of the designed three-arm discriminators.

Discriminator no. 1 can be used for measurements on a 35-GHz gyrotron. The required coupling coefficient is 30 dB, and the radius of the circular main waveguide is 10 mm. Three coupling arms are designed for the TE_{11}, TE_{01}, and TE_{02} modes, respectively. The coupling holes are placed on the common wall between the circular waveguide and the narrow side of the rectangular waveguide. Notice that the TM modes in the main waveguide cannot be coupled into the sub-waveguide in this situation. Table I gives the dimensions and suppressions of all of the unwanted TE modes at the center frequency. Fig. 4 shows the relations of the variations of the coupling coefficients and suppressions with frequency.

For comparison with the wavenumber spectrometer designed by Kasparek and Müller [7], the operating frequency of the second discriminator we designed is 70 GHz for the TE_{01}, TE_{02}, and TE_{03} modes. The designing results are shown in Table I and Fig. 5. It can be seen from Table I that, with the same radius (13.9 mm) of the main waveguide, the length of the coupling region is only 100 mm for discriminator no. 2, but the length is 1200 mm for the wavenumber spectrometer. The defect of the discriminator is that with the increase of the number of the modes needed to be discriminated the number of coupling arms must be increased. Even so, the whole size of the discriminator is much smaller than that of the wavenumber spectrometer.

In Table I, the suppressions to some unwanted modes are not good enough. Since only three main modes were taken into account in our design, the suppressions to some other modes were calculated, but not designed specifically. The suppression to any mode can be improved by adding a group of coupling holes for this mode. Obviously, this will lead to a quick increase of the number of the coupling holes and the length of the discriminator. On the other hand, the magnitudes of the unwanted modes excited in practical systems are much less than those of the three main modes concerned in our design. (The modes concerned in our design are selected according to the degree of the excitation in the system.) At this point, the power of the unwanted modes coupled into the sub-waveguide will be much smaller than that calculated according to their suppressions. Therefore, the imperfection of suppression to some small-magnitude modes does not affect the normal operation of the designed discriminator.

VI. Summary

The design and calibration method of mode discriminators based upon mode-selective coupling has been presented in

this paper. The design examples for the case of equal-intensity coupling show that this method is useful for designing discriminators. Increasing the groups of coupling holes may suppress more unwanted modes and improve the properties of the mode discriminator. This type of discriminator can be used for mode analysis and power measurement for overmoded microwave systems.

It should be noted that, by making use of this method, the operating frequency region of the designed mode discriminator is narrow. Broadening the passband of the mode discriminator requires unequal-intensity or unequal-interval coupling. This problem will be discussed in a future paper.

ACKNOWLEDGMENT

The authors would like to thank Dr. Y. Wei, X. Wu, and P. Zhou, all of the University of Electronic Science and Technology, Chengdu, Sichuan, China, for their kind help during this study.

REFERENCES

[1] W. Wang, M. Xu, and G. Yu, "Mode analysis and distinction of waveguide system" (in Chinese), *Vacuum Electron. Technol.*, no. 1, pp. 1–6, 1993.

[2] M. Thumm, "High-power millimeter-wave mode converter in overmoded circular waveguides using periodic wall perturbations," *Int. J. Electron.*, vol. 57, no. 6, pp. 1225–1246, 1984.

[3] S. H. Gold *et al.*, "High peak power Ka-band gyrotron oscillator experiment," *Phys. Fluids*, vol. 30, no. 7, pp. 2236–2238, July 1987.

[4] V. L. Bratman and G. G. Denisov, "Powerful millimeter-wave generators based on the stimulated Cerenkov radiation of relativistic electron beams," *Int. J. Infrared Millim. Waves*, vol. 5, no. 9, pp. 1311–1332, 1984.

[5] C. T. Iatrou *et al.*, "Design and experimental operation of a 165-GHz, 1.5-MW, coaxial-cavity gyrotron with axial RF output," *IEEE Trans. Plasma Sci.*, vol. 25, pp. 470–479, June 1997.

[6] Z. X. Zhang *et al.*, "Mode analysis of gyrotron radiation by far field measurements," presented at the Int. Infrared and Millimeter Waves Conf., Miami, FL, 1983.

[7] W. Kasparek and G. A. Müller, "The wavenumber spectrometer—An alternative to the directional coupler for multimode analysis in oversized waveguides," *Int. J. Electron.*, vol. 64, no. 1, pp. 5–20, 1988.

[8] H. J. Barkley *et al.*, "Mode purity measurements on gyrotrons for plasma heating at the stellarator W VII-AS," *Int. J. Electron.*, vol. 64, no. 1, pp. 21–28, 1988.

[9] D. S. Stone, "Mode analysis in multimode waveguides using voltage traveling wave ratios," *IEEE Trans. Microwave Theory Tech.*, vol. MTT-29, pp. 91–95, Feb. 1981.

[10] G. Janzen and H. Stickel, "Mode selective directional couplers in overmoded circular waveguides," presented at the Int. Infrared and Millimeter Waves Conf., Miami, FL, 1989.

[11] ——, "Mode selective directional couplers for overmoded waveguide systems," *Int. J. Infrared Millim. Waves*, vol. 5, no. 7, pp. 887–917, 1984.

[12] ——, "Improved directional couplers for overmoded waveguide systems," *Int. J. Infrared Millim. Waves*, vol. 5, no. 10, pp. 1405–1417, 1984.

[13] W. X. Wang, W. Lawson, and V. L. Granatstein, "The design of a mode selective directional coupler for a high power gryroklystron," *Int. J. Electron.*, vol. 65, no. 3, pp. 705–716, 1988.

[14] W. Lawson, M. E. Read, W. X. Wang, and M. Naiman, "Evaluation of directional couplers for high power gyrotrons," *Int. J. Electron.*, vol. 72, no. 5 and 6, pp. 1135–1144.

[15] W. Wang *et al.*, "The design of TM_{on} mode discriminator for high power microwave system" (in Chinese), *Acta Electron.*, vol. 26, no. 3, pp. 123–125, 1998.

[16] H. A. Bethe, "Theory of diffraction by small holes," *Phys. Rev.*, vol. 66, no. 7, 8, pp. 163–182, Oct. 1944.

[17] R. E. Collin, *Foundation for Microwave Engineering*. New York: McGraw-Hill, 1966.

[18] F. Sporleder and H.-G. Unger, *Waveguide Tapers Transitions and Couplers*. Stevenage, U.K.: Peregrinus, 1979.

[19] S. E. Miller, "Coupled wave theory and waveguide applications," *Bell Syst. Tech. J.*, vol. 33, pp. 661–719, 1954.

[20] R. Levy, "Directional couplers," in *Advances in Microwaves*. New York: Academic, 1966, vol. 1, pp. 140–141.

[21] W. Wang, "Improved design of a high power mode selective directional coupler," *Int. J. Electron.*, vol. 76, no. 1, pp. 131–142, 1994.

Wenxiang Wang was born in Jiansu Province, China, on July 24, 1940. He graduated from the Chengdu Institute of Radio Engineering (now the University of Electronic Science and Technology of China (UESTC), Chengdu, Sichuan, China, in 1963.

Since 1963, he has been with the Institute of High Energy Electronics, UESTC. From 1963 to 1978, he was engaged in the field of microwave electronic tubes including traveling-wave tubes (TWTs), continuous wave (CW) magnetrons, forward wave amplifiers, etc. Since 1979, his research activities have been concerned with gyrotrons, high-power microwave tubes, and techniques. From October 1986 to November 1988, he was a Visiting Scholar with the Plasma Research Laboratory, University of Maryland at College Park, where he investigated and designed the high-power mode-selective directional coupler for gyroklystron. He is currently a Professor with UESTC.

Mr. Wang is a Senior Member of the Chinese Institute of Electronics. He is vice chairman of the Chinese Vacuum Electronics Society.

Yubin Gong (M'01) was born in Shandong Province, China, in December 1967. He received the B.S. degree from the Changchun Institute of Optics and Fine Mechanics, Changchun, China, in 1989, and the M.S. and Ph.D. degrees in physical electronics from the University of Electronic Science and Technology of China (UESTC), Chengdu, Sichuan, China, in 1992 and 1998, respectively.

In 1992, he began researching microwave tube and passive microwave devices at UESTC. In 1997, he joined the City University of Hong Kong, as a Visiting Scholar, where he was involved with the measured equation of invariance in time domain. He is currently a Professor with UESTC. He has authored and coauthored over 60 research papers. His research interests include high-power microwave sources, broad-band high-power traveling-wave tubes, and computer simulation of microwave tubes.

Guofen Yu received the B.S. degree in applied physics from the National University of Defense Science and Technology, Changsha, China, in 1987, and the M.S. and Ph.D. degrees in physical electronics from the University of Electronics Science and Technology of China (UESTC), Chengdu, Sichuan, China, in 1990 and 1998, respectively.

Since 1990, she has been involved with microwave techniques and microwave tubes, such as TWTs, gyrotrons, and vircators. From March 1999 to December 2000, she was a Post-Doctoral Associate with the Department of Electrical and Computer Engineering, Old Dominion University, Norfolk, VA, where she was involved with microwave effects on biological cells. She is currently involved with bioelectromagnetics and microwave technology at UESTC.

Lingna Yue, photograph and biography not available at time of publication.

Jiahong Sun, photograph and biography not available at time of publication.